

# (12) EFFECTS OF GLASS FIBER SHEETS ON THE STRENGTHENING OF GFRP BOLTED CONNECTIONS WITH VARIOUS GEOMETRIC PARAMETERS

Phan Viet Nhut<sup>1</sup>, Tran Quang Duc<sup>2</sup>, Yukihiro Matsumoto<sup>3</sup>

<sup>1</sup>Member of JSCE, Graduate student, Dept. of Architecture and Civil Engineering, Toyohashi Uni. of Technology  
(1-1 Hibarigaoka, Tempaku-cho, Toyohashi, Aichi, 441-8580, Japan)  
E-mail: [phan.viet.nhut.yu@tut.jp](mailto:phan.viet.nhut.yu@tut.jp)

<sup>2</sup>Member of JSCE, Graduate student, Dept. of Architecture and Civil Engineering, Toyohashi Uni. of Technology  
(1-1 Hibarigaoka, Tempaku-cho, Toyohashi, Aichi, 441-8580, Japan)  
E-mail: [tran.quang.duc.wq@tut.jp](mailto:tran.quang.duc.wq@tut.jp)

<sup>3</sup>Member of JSCE, Assoc. Professor, Dept. of Architecture and Civil Engineering, Toyohashi Uni. of Technology  
(1-1 Hibarigaoka, Tempaku-cho, Toyohashi, Aichi, 441-8580, Japan)  
E-mail: [y-matsum@ace.tut.ac.jp](mailto:y-matsum@ace.tut.ac.jp)

Pultruded glass fiber reinforced polymer (PGFRP) profiles have been used increasingly in the civil engineering field and infrastructure applications because they offer many advanced properties such as low density, high strength, high corrosion resistance, and a wide variety of shapes. The popular applications of PGFRP can be found in the construction of bridges, housing, and office buildings. However, the PGFRP profiles, which containing main glass roving parts, usually lack shear strength because the shear strength of the PGFRP profiles is mainly dependent on the matrix shear strength. To overcome this problem, thin multiaxial glass fiber sheets (GFSs) molded by VaRTM methods can be effectively used to strengthen the GFRP connections. In this study, the effects GFSs on the strengthening of single bolted PGFRP connections were experimentally investigated under tensile shear tests. Various geometric parameters of GFRP bolted connections with different bolted end and side distances were discussed in the results. Three types of GFSs ( $0^\circ/90^\circ$  GFSs,  $\pm 45^\circ$  GFSs, and chopped strand mat GFSs) were used to strengthen the connections. The results showed that the strengthening effects were decreased as the increase in end-edge distances of the connections for all types of the GFSs. Moreover, the strengthening effects of the three types of GFSs were different depending on the values of the ratios between the widths of the connections to the bolt diameters.

**Key Words :** GFRP, failure modes, bolted connection, strengthening, ultimate loads, glass fiber sheets

## 1. Introduction

Because of many outstanding characteristics such as flexibility, high strength, and chemical resistance, glass fiber reinforced polymers (GFRPs) have been used widely in bridge and building construction [1–3]. GFRPs can consist of various forms of glass fiber reinforcements, including glass roving, chopped strands, fabrics, and mats. In the civil construction field, the pultrusion is an easy method to create the various section areas of GFRP load-bearing products. Pultruded GFRP (PGFRP) profiles have attracted the attention of designers due to many of their excellent characteristics such as low density, high weight ratio and strength, high corrosion resistance, low heat transmission, and a wide variety of shapes. The applications of PGFRPs are found in the construction of bridges, housing, and office buildings [4–5].

In civil engineering fields, bolted connections are used widely for

PGFRP connections because this is an easy way to connect PGFRP members. Five main failure modes can be found in bolted GFRP connections: fastener shear failure, bearing failure, net-tension failure, cleavage failure, and shear-out failure. The modes of failure highly depend on specimen geometries and laminations. Shear-out failure occurs if the ratio between the end distance from the edge to bolt center ( $e$ ) and the bolt diameter ( $d$ ) is small, net-tension failure occurs with the small ratio between the width of the specimen ( $w$ ) and the bolt diameter ( $d$ ), and bearing failure appears with an adequately large  $e$  and  $w$ . The failure modes of PGFRP are also depended on the loading direction or the angles of fiber and loading directions. The usual type of PGFRP contains a unidirectional inside glass roving part and an outside glass fiber mat/chopped strand mat. Shear-out failure can easily occur in this type of configuration if the ratio  $e/d$  is small, and the loading direction is the same as the direction of the unidirectional glass roving. This is because the shear strength of the PGFRP profiles in the glass roving

direction is mainly dependent on the matrix shear strength. To increase the application possibilities of PGFRP members, the bolted PGFRP connections need higher shear strength to improve the ductility of PGFRP profiles in the civil engineering field. A strengthening method for PGFRP connections using glass fiber sheets (GFSs) with a single bolt was reported earlier in [6] with a 16 mm bolt diameter.

In this study, the effects GFSs on the strengthening of single bolted PGFRP connections were experimentally investigated under tensile shear tests. Various geometric parameters of GFRP bolted connections with different bolt-end and bolt-side distances were discussed in the results. Flat PGFRP specimens were cut from C150 products (a product of AGC Matex Co., Ltd., Japan) and used for the connections with pin-bearing single bolts. These profiles are composed of two parts: inner unidirectional glass roving and outer glass fiber mat. The GFSs created by the Vacuum-assisted Resin Transfer Molding (VaRTM) method were used to reinforce the PGFRP connections. Three types of GFSs ( $0^\circ/90^\circ$  and  $\pm 45^\circ$  glass-woven roving, and chopped strand mat (CSM)) were used for the strengthening of the PGFRP connections. The tension load was applied in the direction of the glass roving part because shear strength is small in this direction.

## 2. Specimen preparation

### (1) PGFRP profiles and GFSs

The PGFRP profiles, namely PLALLOY C150 (products of MOLYMER MATEX Co., Ltd., Japan) were used for making the specimens. The sectional areas of C150 profiles include glass fiber mat parts (GFM), unidirectional glass roving parts (UD), and unsaturated polyester resin. The average thickness of PGFRP channels is 5 mm with a total of 4.2mm thickness for the UD part and 0.8mm thickness for the GFM part. The main parts in the webs of the PGFRP channels were cut for making the specimens of the tensile tests.

In this investigation, three types of GFSs,  $0^\circ/90^\circ$  GFSs,  $\pm 45^\circ$  GFSs, and CSM GFSs were employed. Every type of strengthening GFS has 6 lamina layers. The average thickness of  $0^\circ/90^\circ$  ( $\pm 45^\circ$ ) GFSs and CSM GFSs were around 0.38mm/layer and 0.46mm/layer, respectively.  $0^\circ/90^\circ$  GFSs were molded from two-directional  $0^\circ/90^\circ$  woven roving (ERW580-554A),  $\pm 45^\circ$  GFSs were cut by the rotations of  $0^\circ/90^\circ$  GFSs with the angles of  $45^\circ$ . CSM GFSs were fabricated from a multi-axial chopped strand mat (ECM450-501). CSM sheets can be considered as in-plane isotropic material because the fibers are short and have various directional orientations. Both  $0^\circ/90^\circ$  woven roving and CSM are products of Central Glass Co., Ltd., Tokyo, Japan. The CSM and  $0^\circ/90^\circ$  woven roving have weights of  $450 \text{ (g/m}^2\text{)}$  and  $580 \text{ (g/m}^2\text{)}$ , respectively. All GFSs were molded by the VaRTM method from fiber sheets with pregnant resin, E205 (Konishi, Osaka, Japan). The GFSs were cut and bonded to both sides of the PGFRP plates using E250 adhesive. The bonded specimens then were kept for

curing around one week before drilling the holes. Fig. 1 shows the PGFRP plates, GFSs, and the final specimens after bonded with GFSs and hole drilling.

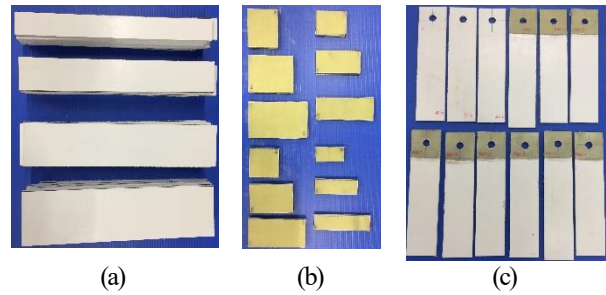


Fig. 1. Specimen preparation: (a) PGFRP, (b) GFSs, and (c) specimens with drilling holes

### (2) Specimen configuration

In this study, various geometric parameters of GFRP bolted connections with and without GFS strengthening were analyzed. The specimens had different values of the ratios between the width to the bolt diameter ( $w/d$ ) and ratios between the end distances to the bolt diameter ( $e/d$ ). Four types of values of  $w/d$  (2, 3, 4, 5) and three types of values of  $e/d$  (2,3,5) were used for the investigations. All specimens used the bolt diameter  $d = 16\text{mm}$ . Fig. 2 shows the specimen configurations and Table 1 shows the specimen notations of the specimens. There were three specimens for every parameter of the specimens, therefore, a total of 144 specimens were tested by the experiments.

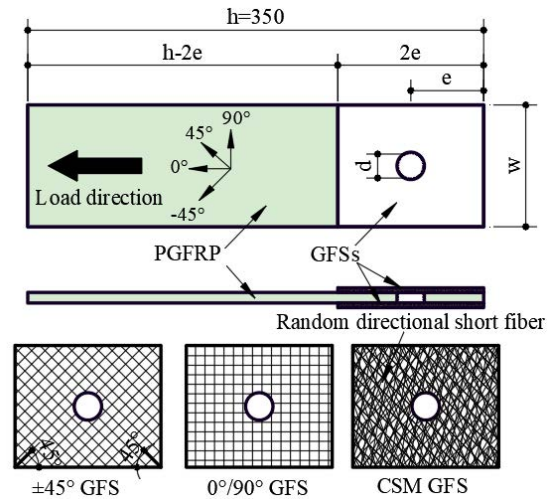


Fig. 2. Specimen configurations. Unit: mm

Table 1. Specimen notation of the specimen

[NS] <sub>ab</sub>	NS: Non-strengthened specimen
[A] <sub>ab</sub>	A: Specimen strengthened by type A of GFSs
a = $w/d$	(A includes $\pm 45^\circ$ GFS (45), $0^\circ/90^\circ$ GFS (090), or CSM GFS (CSM))
b = $e/d$	

## 3. Experimental setup

The bearing tests of the PGFRP connections were carried out using a 1000 kN Maekawa tensile testing machine (Maekawa Testing Machine MFG Co., Ltd., Tokyo, Japan), as shown in Fig. 3. Tensile

loads were applied in the direction of glass roving ( $0^\circ$  according to Fig. 2) because the shear strength was weak in this direction. Two displacement transducers were assembled to measure the relative displacements of the connections.

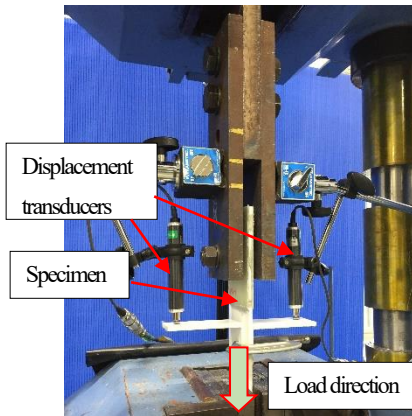


Fig. 3. Test setup

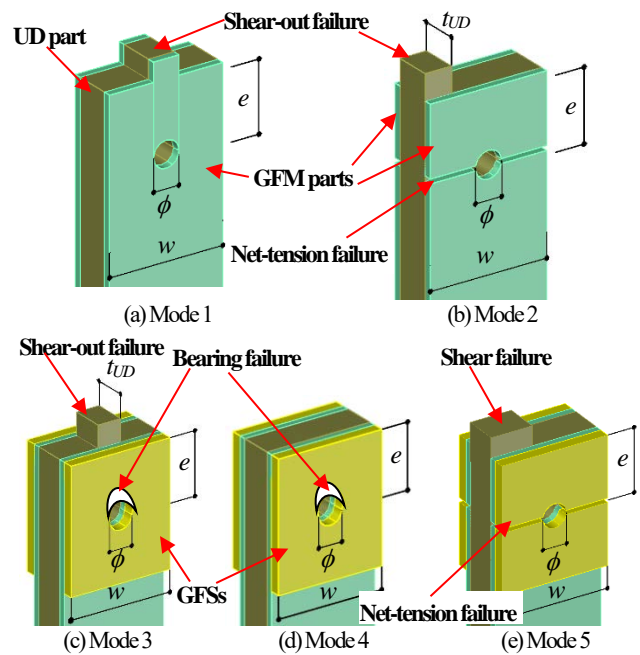


Fig. 4. Typical failure modes of the specimens

## 4. Results and discussion

### (1) Failure modes of the specimens

Fig. 4 explains of failures modes of PGFRP connections. Because of orthotropic materials, the failure modes of PGFRP connections are relatively complex. These failure modes are different from the failure modes of isotropic materials, e.g., steel. After strengthening with the GFSs, the failure modes of PGFRP connections are combinations of some failure modes of isotropic materials such as shear-out failure, bearing failure, net-tension failure, and shear failure. The types of PGFRP connection failure modes depend on the stacking of lamina components such as PGFRP and GFSs. Different failure modes were found with different values of  $w/d$  and  $e/d$ . Mode 1 and Mode 2 are found in non-strengthened specimens (NS specimens). Mode 1 is a shear-out failure in the whole thicknesses of the connections, whereas Mode 2 is the combination of shear failure in the UD part and net-tension failure in the GFM part. After being strengthened with GFSs, the failure modes of the connections can be changed from Mode 1 and 2 to Mode 3, 4, 5 depending on the geometries of the connections. Mode 3 is the combination of shear-out failure in the UD part and bearing failures in the GFM part and GFS part. Mode 4 occurred with enough lengths of  $e$  and  $w$ , where all bearing failures occurred in all parts of the connections. Mode 5 is the combination of shear failure in the UD part and net-tension failures in the GFM part and GFS part. Mode 5 could be found with small values of  $w$ , suitable lengths of  $e$ , and using CSM GFS for the strengthening. Mode 3 was a typical failure mode for the strengthened specimens when Mode 4 and Mode 5 did not occur in the connections.

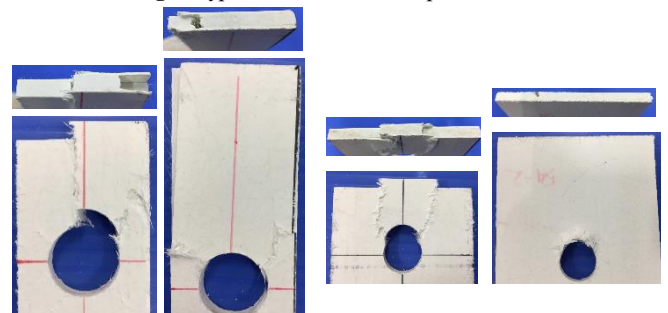


Fig. 5. Some experimental failure modes of the non-strengthened specimens

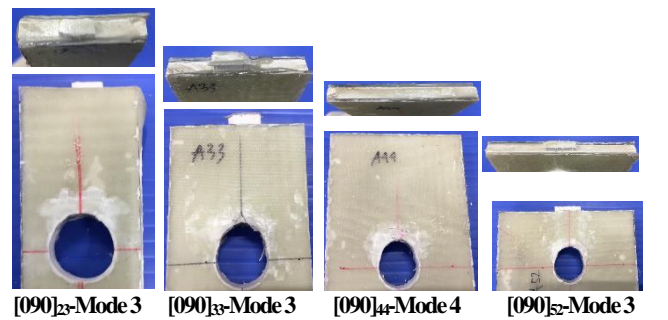


Fig. 6. Some experimental failure modes of the specimens strengthened by  $0^\circ/90^\circ$  GFSs

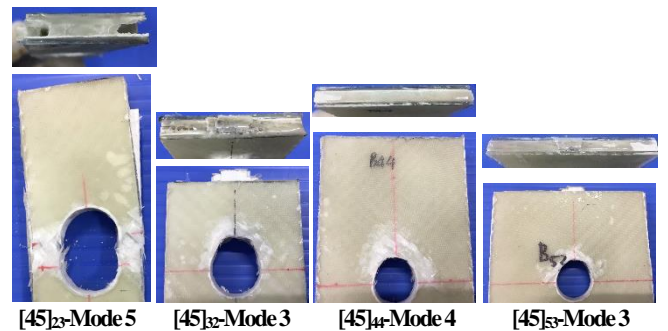


Fig. 7. Some experimental failure modes of the specimens strengthened by  $\pm 45^\circ$  GFSs

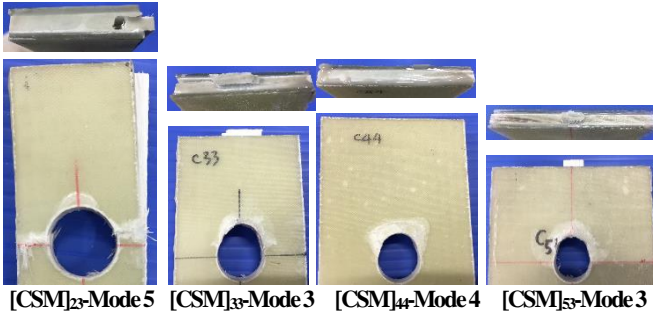


Fig. 8. Some experimental failure modes of the specimens strengthened by CSM GFSs

Table 2. Experimental failure modes of specimens having  $w/d=2$

Specimen	FM	Specimen	FM	Specimen	FM
[NS] <sub>22</sub>	M1	[NS] <sub>23</sub>	M2	[NS] <sub>24</sub>	M2
[0/90] <sub>22</sub>	M3	[0/90] <sub>23</sub>	M3	[0/90] <sub>24</sub>	M3
[45] <sub>22</sub>	M5	[45] <sub>23</sub>	M5	[45] <sub>24</sub>	M5
[CSM] <sub>22</sub>	M5	[CSM] <sub>23</sub>	M5	[CSM] <sub>24</sub>	M5

Table 3. Experimental failure modes of specimens having  $w/d=3$

Specimen	FM	Specimen	FM	Specimen	FM
[NS] <sub>32</sub>	M1	[NS] <sub>33</sub>	M1	[NS] <sub>34</sub>	M4
[0/90] <sub>32</sub>	M3	[0/90] <sub>33</sub>	M3	[0/90] <sub>34</sub>	M4
[45] <sub>32</sub>	M3	[45] <sub>33</sub>	M3	[45] <sub>34</sub>	M4
[CSM] <sub>32</sub>	M3	[CSM] <sub>33</sub>	M3/M4	[CSM] <sub>34</sub>	M4

Table 4. Experimental failure modes of specimens having  $w/d=4$

Specimen	FM	Specimen	FM	Specimen	FM
[NS] <sub>42</sub>	M1	[NS] <sub>43</sub>	M1	[NS] <sub>44</sub>	M4
[0/90] <sub>42</sub>	M3	[0/90] <sub>43</sub>	M3	[0/90] <sub>44</sub>	M4
[45] <sub>42</sub>	M3	[45] <sub>43</sub>	M3	[45] <sub>44</sub>	M4
[CSM] <sub>42</sub>	M3	[CSM] <sub>43</sub>	M3/M4	[CSM] <sub>44</sub>	M4

Table 5. Experimental failure modes of specimens having  $w/d=5$

Specimen	FM	Specimen	FM	Specimen	FM
[NS] <sub>52</sub>	M1	[NS] <sub>53</sub>	M1	[NS] <sub>54</sub>	M4
[0/90] <sub>52</sub>	M3	[0/90] <sub>53</sub>	M3	[0/90] <sub>54</sub>	M4
[45] <sub>52</sub>	M3	[45] <sub>53</sub>	M3	[45] <sub>54</sub>	M4
[CSM] <sub>52</sub>	M3	[CSM] <sub>53</sub>	M3/M4	[CSM] <sub>54</sub>	M4

Figs. 5, 6, 7, and 8 show the typical experimental failure modes of the specimens. Tables 2 to 5 show the experimental failure modes of the specimens obtained from the tests. In Tables 2 to 5, FM is the notation of failure mode, M1 to M5 are the notations of Mode 1 to Mode 5 failures. It can be seen from the tables that Mode 2 failure occurred in the non-strengthened PGFRP specimens having small values of  $w/d$  ( $w/d=2$ ) and large values of  $e/d$  ( $e/d \geq 3$ ), e.g., specimens [NS]<sub>23</sub> and [NS]<sub>24</sub>. Mode 4 occurred in the non-strengthened specimens with simultaneous large enough values of  $w/d$  and  $e/d$  ( $w/d \geq 3$  and  $e/d \geq 4$ ), e.g., specimens [NS]<sub>34</sub>, [NS]<sub>44</sub>, and [NS]<sub>54</sub>. Mode 1 failure occurred in the non-strengthened specimens, in which Mode 2 and Mode 4 did not occur. After being strengthened with GFSs, the failure modes of specimens changed. Because of the lack of shear

strengths in the UD parts, the main failure modes of the connections are Mode 3, where shear-out failures occurred in the UD parts. Mode 4 failures can be found in the strengthened specimens with simultaneous large enough values of  $w/d$  and  $e/d$  ( $w/d \geq 3$  and  $e/d \geq 4$ ). When the widths of the specimens were small ( $w/d = 2$ ), the failure modes of the specimens were Mode 5, excluding the specimens strengthened by  $0^\circ/90^\circ$  GFSs. CSM GFSs have the smallest shear strengths [7] compared with  $\pm 45^\circ$  and  $0^\circ/90^\circ$  GFSs, therefore, net-tension failures easily occur with small tensile areas. On the other hand, although the shear strength of  $0^\circ/90^\circ$  GFS is smaller than that of  $\pm 45^\circ$  GFS, the discontinuation of the fibers in  $\pm 45^\circ$  GFS by cutting has significant effects on the shear strength of  $\pm 45^\circ$  GFS and reduce the practical shear strength of  $\pm 45^\circ$  GFS, especially when the sectional area is small. That is the reason net-tension also occurred in the  $\pm 45^\circ$  GFSs when they have small values of  $w/d$ . If Mode 5 occurs in the connection, net-tension failure occurs first in the GFS parts, the connections are then bent by the local failures of the fibers in GFSs. This bending causes the shear failures in the UD parts in one side or two sides around the bolt holes in the load directions.

## (2) Strengthening effect of GFSs on the connection strength

Tables 6 to 9 show the maximum failure loads of all the specimens and the strengthening effects of the GFSs on the ultimate loads of PGFRP connections. In the tables,  $P_{st}$  is the maximum load of the strengthened specimen and  $P_{NS}$  is the maximum load of the non-strengthened specimen. Overall, the use of strengthening GFSs could effectively increase the maximum failure loads of the PGFRP connections, around from 1.7 to 2.9 times higher depending on the types of GFSs and specimen configurations. It should be noted that the total thickness of strengthening GFSs was only around half the value of PGFRP thickness.

The strengthening effects of all three types of GFSs were higher if the connections had smaller values of  $e/d$ . For example, the strengthening effects of GFSs for the connections having the ratios  $e/d = 2$  were around from 120% to 191%, while these values for the connections having the ratios  $e/d = 3$  and  $e/d = 5$  were around from 77% to 123% and from 64% to 93%, respectively. The reason for this trend is shear-out failure easier occurs for the connections having small values of  $e/d$ . The GFSs could effectively constrain the shear-out failures of the PGFRP connections. Although the final failure modes were also shear-out failures in the UD parts ( $e/d = 2$  and  $e/d = 3$  specimens), the GFSs had good effects on the delay of the appearances of shear-out failures in the UD parts. The shear-out failures occurred very early in the non-strengthened specimens with small values of  $e/d$ . As a result, the maximum failure loads of the connections having small values of  $e/d$  were increased remarkably.

**Table 6.** Average loads and strengthening effects of GFSs on the specimens having  $w/d=2$

Specimen	[NS] <sub>22</sub>	[0/90] <sub>22</sub>	[45] <sub>22</sub>	[CSM] <sub>22</sub>	[NS] <sub>23</sub>	[0/90] <sub>23</sub>	[45] <sub>23</sub>	[CSM] <sub>23</sub>	[NS] <sub>24</sub>	[0/90] <sub>24</sub>	[45] <sub>24</sub>	[CSM] <sub>24</sub>
Average load (kN)	6.92	17.36	16.34	18.10	11.82	23.71	21.67	20.97	14.84	26.81	24.41	25.11
Pst/P <sub>NS</sub>		2.51	2.36	2.62		2.01	1.83	1.77		1.81	1.64	1.69
Strengthening effect (%)		151%	136%	162%		101%	83%	77%		81%	64%	69%

**Table 7.** Average loads and strengthening effects of GFSs on the specimens having  $w/d=3$

Specimen	[NS] <sub>32</sub>	[0/90] <sub>32</sub>	[45] <sub>32</sub>	[CSM] <sub>32</sub>	[NS] <sub>33</sub>	[0/90] <sub>33</sub>	[45] <sub>33</sub>	[CSM] <sub>33</sub>	[NS] <sub>34</sub>	[0/90] <sub>34</sub>	[45] <sub>34</sub>	[CSM] <sub>34</sub>
Average load (kN)	6.78	16.72	17.82	19.71	13.45	24.21	24.22	27.65	15.55	26.37	28.04	28.85
Pst/P <sub>NS</sub>		2.47	2.63	2.91		1.80	1.80	2.06		1.70	1.80	1.86
Strengthening effect (%)		147%	163%	191%		80%	80%	106%		70%	80%	86%

**Table 8.** Average loads and strengthening effects of GFSs on the specimens having  $w/d=4$

Specimen	[NS] <sub>42</sub>	[0/90] <sub>42</sub>	[45] <sub>42</sub>	[CSM] <sub>42</sub>	[NS] <sub>43</sub>	[0/90] <sub>43</sub>	[45] <sub>43</sub>	[CSM] <sub>43</sub>	[NS] <sub>44</sub>	[0/90] <sub>44</sub>	[45] <sub>44</sub>	[CSM] <sub>44</sub>
Average load (kN)	7.22	16.63	16.51	19.75	12.79	25.02	25.54	27.58	14.74	26.87	27.98	28.50
Pst/P <sub>NS</sub>		2.30	2.29	2.74		1.96	2.00	2.16		1.82	1.90	1.93
Strengthening effect (%)		130%	129%	174%		96%	100%	116%		82%	90%	93%

**Table 9.** Average loads and strengthening effects of GFSs on the specimens having  $w/d=5$

Specimen	[NS] <sub>52</sub>	[0/90] <sub>52</sub>	[45] <sub>52</sub>	[CSM] <sub>52</sub>	[NS] <sub>53</sub>	[0/90] <sub>53</sub>	[45] <sub>53</sub>	[CSM] <sub>53</sub>	[NS] <sub>54</sub>	[0/90] <sub>54</sub>	[45] <sub>54</sub>	[CSM] <sub>54</sub>
Average load (kN)	7.65	16.80	16.59	19.26	12.47	23.52	22.60	27.77	16.14	28.14	27.93	28.54
Pst/P <sub>NS</sub>		2.20	2.17	2.52		1.89	1.81	2.23		1.74	1.73	1.77
Strengthening effect (%)		120%	117%	152%		89%	81%	123%		74%	73%	77%

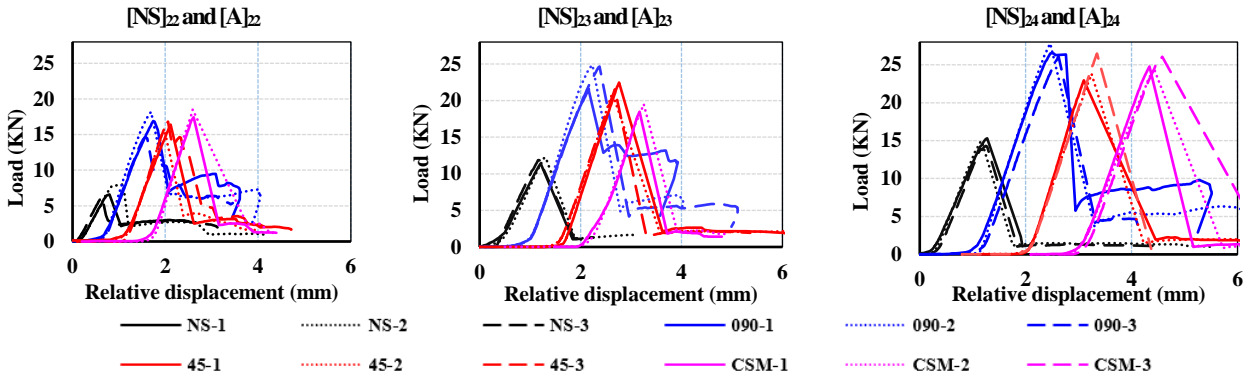


**Fig. 9.** Load–relative displacement relations of the specimens having  $w/d=2$

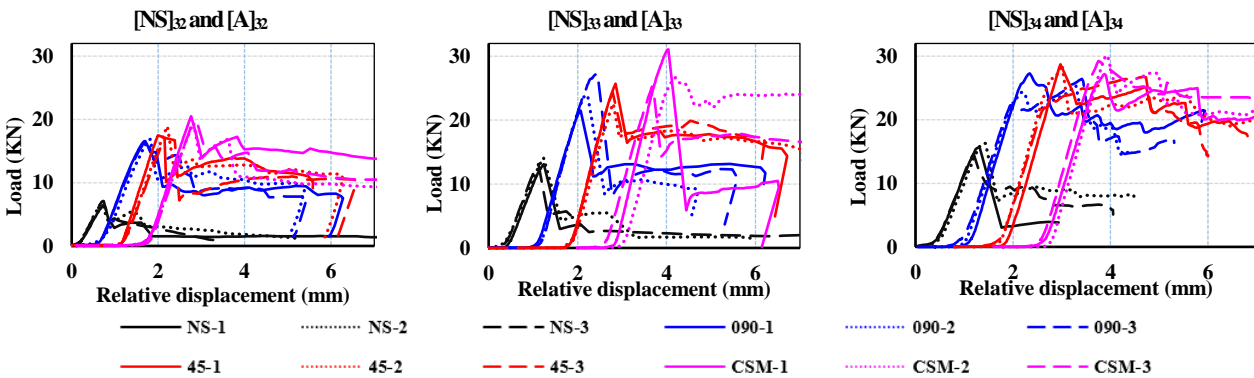


**Fig. 10.** Load–relative displacement relations of the specimens having  $w/d=3$

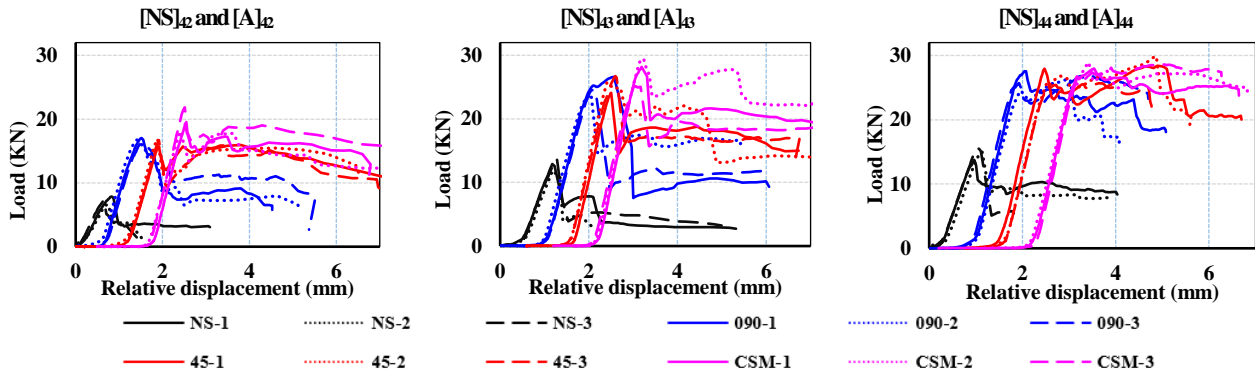


Fig. 11. Load–relative displacement relations of the specimens having  $w/d=4$

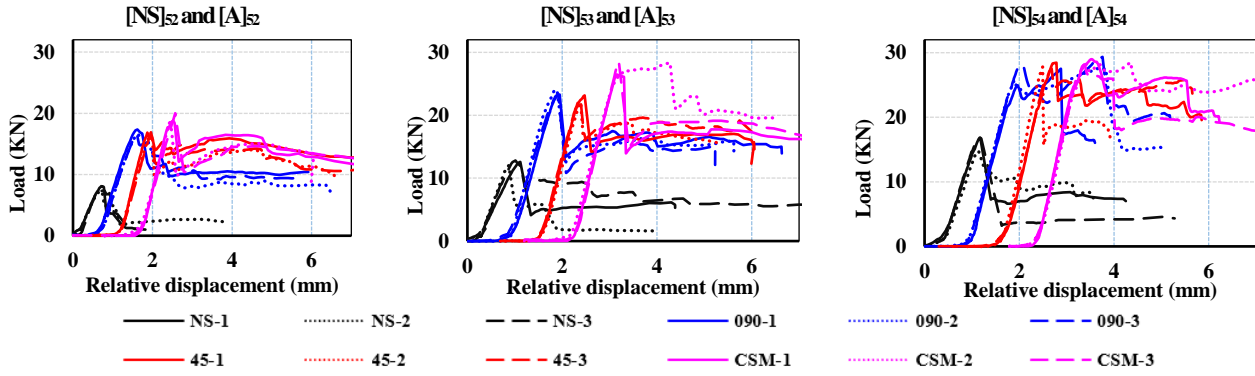


Fig. 12. Load–relative displacement relations of the specimens having  $w/d=5$

In the cases of the specimens having the ratios  $e/d=4$ ,  $w/d=2$ , and using  $0^\circ/90^\circ$  GFSs, the end-distances were large enough to delay the shear-out failures in UD parts. The  $0^\circ/90^\circ$  GFSs, in this case, had more meaning on the contributions of bearing strengths than on the prevention of the shear-out failures in UD parts. When using  $\pm 45^\circ$  GFSs or CSM GFSs and connections having the ratios  $e/d=4$  and  $w/d=2$ , the GFSs were damaged first by the net-tension failures, then shear failures occurred in the UD parts. Therefore, GFSs in these cases did not have many effects on the prevention of shear-out failures in the UD parts. In other cases when the specimens have the ratios  $e/d=4$  and  $w/d \geq 3$ , because all bearing failures occurred in the connections, the GFSs in these cases have meaning on the contributions of bearing strengths of the connections.

The effects of the ratios  $w/d$  on the connection strengths were not significant if ratios  $w/d$  were equal or greater than 3 ( $w/d \geq 3$ ). When changing  $w/d$  from 3 to 4 and 5, the failure modes of non-strengthened specimens were the same with the same values of  $e/d$ . The same situations of failure modes occurred with strengthened specimens.

If the connection failure was Mode 3, the connection strengths depend on the shear-out strengths of UD parts and bearing strengths of GFM parts and GFS parts. Because shear-out strengths only depended on the end-distances and bearing strengths did not depend on the widths of the specimens, the strengthening effects of GFSs on the ultimate loads of the connections having  $w/d \geq 3$  and same end-distance were not significant when Mode 3 or Mode 4 failure occurred

in these connections. For example, the ultimate loads of  $[0/90]_{32}$ ,  $[0/90]_{42}$ , and  $[0/90]_{52}$  specimens 16.72 (kN), 16.63 (kN), and 16.80 (kN), respectively; these values of  $[0/90]_{33}$ ,  $[0/90]_{43}$ , and  $[0/90]_{53}$  specimens were 24.21 (kN), 25.02 (kN), and 23.52 (kN), respectively; and the values for  $[0/90]_{34}$ ,  $[0/90]_{44}$ , and  $[0/90]_{54}$  specimens were 26.37 (kN), 26.87 (kN), and 28.14 (kN), respectively. The ultimate loads of the connections, which are strengthened by  $\pm 45^\circ$  GFSs and CSM GFSs with  $w/d \geq 3$  had the same trends as the  $0^\circ/90^\circ$  GFS-strengthened connections. The specimens having the same types of GFS strengthening, same values of  $e/d$  but different values of  $w/d$  experienced the variations of the strengthening effects, as shown in Tables 6 to 9. It can be seen that these variations of the strengthening effects are because the strengthening effects were calculated according to the differences with the non-strengthened specimens. However, the ultimate failure loads of non-strengthened specimens with the same failure modes were different, e.g., specimens  $[NS]_{34}$ ,  $[NS]_{44}$ , and  $[NS]_{54}$  with the failure loads 15.55 (kN), 14.74 (kN), and 16.14 (kN), respectively. These different failure loads could come from the un-uniform in PGFRP material quality or the effects of drilling holes during the preparations of the specimens. As a result, the strengthening effects were changed in the specimens having different values of  $w/d$  (same values of  $e/d$ ) even though the ratios  $w/d$  did not affect significantly the connection strengths when  $w/d \geq 3$ .

The effects of ratios  $w/d$  on the failure modes of the specimens can be seen when changing the ratios from  $w/d=2$  to  $w/d \geq 3$ . The changes

of failure modes of the connections resulted in the difference in the strengthening effects of the GFSs, especially specimens having  $e/d \geq 3$  and  $w/d=2$ . Because the failures occurred first in the  $\pm 45^\circ$  GFSs and CSM GFSs (Mode 5), the strengthening effects of specimens strengthened by  $\pm 45^\circ$  GFSs and CSM GFSs were smaller than those strengthened by  $0^\circ/90^\circ$  GFSs (101% in [0/90]<sub>23</sub>, 83% in [045]<sub>23</sub>, and 77% in [CSM]<sub>23</sub> specimens; 81% in [0/90]<sub>24</sub>, 64% in [045]<sub>24</sub>, and 69% in [CSM]<sub>24</sub> specimens).

Of all three types of GFSs, CSM GFSs proved the best and stable strengthening effects than  $\pm 45^\circ$  GFSs and  $0^\circ/90^\circ$  GFSs, excluding the [CSM]<sub>23</sub> and [CSM]<sub>24</sub> specimens with different failure modes.  $0^\circ/90^\circ$  GFSs and  $\pm 45^\circ$  GFSs are continuous fiberglass roving, they are sensitive to the local damages caused by the drilling holes. Moreover, the continuation of the glass fiber in  $\pm 45^\circ$  GFSs and  $0^\circ/90^\circ$  GFSs was also disconnected by drilling. These problems caused the decrease in the strengthening effects of GFSs in single bolted PGFRP connections. On the other hand, CSM GFSs were original short random directional fibers, therefore, the drilling had small effects on the local failures of the fibers, making the strengthened specimens had more stable results.

Figs. 9 to 12 show the load–relative displacement relations obtained from the experiments. The relative displacements were average values calculated from two displacement transducers, shown in Fig. 3. There are several behaviors of the load–relative displacement relations with different values of  $e/d$  and  $w/d$ . In the cases of non-strengthened specimens (except for specimens [NS]<sub>34</sub>, [NS]<sub>44</sub>, and [NS]<sub>54</sub> with Mode 4 failures), the loading decreased rapidly after reaching the maximum loads and the connections almost lost all the bearing capacities. The decrease of loads after reaching the maximum loads also can be found in specimens [NS]<sub>34</sub>, [NS]<sub>44</sub>, and [NS]<sub>54</sub>. However, these connections could still bear a little load because all bearing failures occurred in the connections. If the local failures were severe in the connections, the loads would decrease greatly and the connections failed to continue bearing loads, e.g., specimens [NS]<sub>34</sub>-1, [NS]<sub>44</sub>-3, and [NS]<sub>54</sub>-3. It can be found in Figs. 9 to 12 that the behaviors of the load–relative displacement relations were also different in strengthened specimens with different values of  $w/d$ . If the ratios  $w/d$  were smallest ( $w/d=2$ ), all the loads decreased quickly, and the connections were lost the bearing capacities. When increasing the values of  $w/d$  ( $w/d \geq 3$ ), better behaviors were seen in the strengthened specimens. The main failure modes of strengthened specimens with  $w/d \geq 3$  and  $e/d < 4$  were Mode 3 where shear-out failures occurred in the UD parts and bearing failures experienced in the GFSs. In these cases, loads were reduced around half after reaching the maximum values. The reduction of the load is because the shear-out failure occurred in the UD part. Then, GFSs could bear the remaining loads while the displacements continued to develop. The best performances were found in the strengthened specimens with  $w/d \geq 3$  and  $e/d=4$ . All bearing failures occurred in the connections and this type of failure was

the best for the ductility performance of the PGFRP connection.

## 5. Conclusion

This study focused on the investigations of the strengthening effects of GFSs on the connection strengths of single bolted PGFRP connections. Various geometric parameters of PGFRP connections with different bolt–end distances and bolt–side distances were experimentally investigated. Some main points are highlighted as follows.

- The failure modes of non-strengthened specimens can be all bearing failure – Mode 4 ( $w/d \geq 3$  and  $e/d \geq 4$ ), a combination of shear-out failure in the UD part and net-tension failure in GFM– Mode 2 ( $w/d=2$  and  $e/d \geq 3$ ), or all shear-out failure – Mode 1 (other cases). After being strengthened with GFSs, the failure modes of specimens changed. Mode 3 failures, in which the shear-out failure occurred in the UD part and bearing failure occurred in the GFS and GFM, could be found in many specimens. Mode 4 failures can be found in the strengthened specimens with simultaneous large enough values of  $w/d$  and  $e/d$  ( $w/d \geq 3$  and  $e/d \geq 4$ ). When the widths of the specimens were small ( $w/d=2$ ), the failure modes of the specimens were Mode 5, excluding the specimens strengthened by  $0^\circ/90^\circ$  GFSs.

- GFSs could effectively increase the maximum failure loads of the PGFRP connections, around from 1.7 to 2.9 times higher depending on the types of GFSs and specimen configurations.

- The strengthening effects of all three types of GFSs were higher if the connections had smaller values of  $e/d$ . In this study, the strengthening effects of all types of GFSs were highest with connections having  $e/d=2$ . These effects were decreased with the increase of bolt–end distances.

- The effects of ratios  $w/d$  on the failure modes of the specimens can be seen when changing the ratios from  $w/d=2$  to  $w/d \geq 3$ . The effects of the ratios  $w/d$  on the connection strengths were not significant if ratios  $w/d$  were equal or greater than 3 ( $w/d \geq 3$ ).

- Of all three types of GFSs, CSM GFSs proved the best and stable strengthening effects than  $\pm 45^\circ$  GFSs and  $0^\circ/90^\circ$  GFSs, excluding the specimens having small values of  $w/d$  ( $w/d=2$ ).

- GFSs have important roles in the keeping of bearing loads for PGFRP connections after maximum failure loads when the specimens having  $w/d \geq 3$ . The best performances were found in the strengthened specimens with  $w/d \geq 3$  and  $e/d=4$ . All bearing failures occurred in the connections and this type of failure was the best for the ductility performance of the PGFRP connection.

## References

- 1) Keller, T.: Use of fiber reinforced polymers in bridge construction. Structural engineering documents. Int Assoc Bridge Struct Eng IABSE.

- 131, ISBN 3-85748-108-0 (2003).
- 2) Sathishkumar, T.P., et al.: Glass fiber-reinforced polymer composites – a review. *J Reinf Plast Comp.* 33, 1258-1275 (2014).
  - 3) Ali, H.T., et al.: Fiber reinforced polymer composites in bridge industry. *Structures.* 30, pp. 774-785 (2021).
  - 4) Correia, J.R., et al.: A review of the fire behaviour of pultruded GFRP structural profiles for civil engineering applications. *Compos Struct.* 127, pp. 267-287 (2015).
  - 5) Green, A., et al.: Pultruded Reinforced Plastics for Civil Engineering Structural Applications. *J Reinf Plast Comp.* 13, pp. 942-951 (1994).
  - 6) Nhut, P.V., et al.: Improving the Shear Strength of Bolted Connections in Pultruded GFRP using Glass Fiber Sheets. *Compos Struct.* 255, 112896 (2021).
  - 7) Nhut, P.V., et al.: On the Strengthening of Pultruded GFRP Connections using Glass Fiber Sheets: A study on the influence of bolt diameter. *Appl. Compos. Mater.* (2021)(Accepted)

(Received September 10, 2021)